RSC Advances

PAPER

View Article Online
View Journal | View Issue

Cite this: *RSC Adv.*, 2025, **15**, 46664

Multicompartmentalized microreactors based on Pickering emulsions for continuous-flow oxidation of primary benzylic alcohols

Yixuan He *

Received 1st August 2025
Accepted 31st October 2025

DOI: 10.1039/d5ra05598a

rsc.li/rsc-advances

A novel system based on Pickering emulsions for the continuous-flow oxidation of primary benzylic alcohols to aldehydes is presented. In this system, transition-metal nanoparticles supported on surface-modified silica nanoparticles serve as both the emulsifier and the active catalyst. Utilizing hydrogen peroxide as a green and renewable oxidant, the system operates continuously under mild conditions, achieves high conversion rates in a short time, and produces minimal, environmentally benign byproducts.

1 Introduction

The oxidation of alcohols to carbonyl compounds has attracted sustained interest. This is largely due to the stability and availability of the alcohol precursors. In addition, the resulting carbonyl products, such as aldehydes, ketones, and carboxylic acids, are highly valuable.[1] These compounds serve as crucial intermediates in the synthesis of pharmaceuticals, industrial feedstocks, and fine chemicals.[2] However, traditional oxidants used for this transformation, such as hexavalent chromium compounds,[3] hypervalent iodine reagents,[4] and activated dimethyl sulfoxide reagents,[5] are typically toxic, expensive, and hazardous. These oxidants often generate substantial waste and byproducts, thereby compromising atom economy and raising serious environmental concerns. In contrast, renewable oxidants, such as oxygen (from air), hydrogen peroxide, and sodium hypochlorite, offer advantages including low cost and minimal byproduct formation.[6] Nevertheless, practical limitations have hindered the widespread adoption of some of these oxidants: air is difficult to handle due to its gaseous nature, while sodium hypochlorite requires strongly alkaline conditions that can degrade sensitive substrates. Among these, hydrogen peroxide stands out as a particularly attractive option due to its favorable balance of cost, renewability, and ease of handling.[7] Unlike sodium hypochlorite, which typically has a low concentration (8–15%), generates large quantities of salt byproduct, and is strongly alkaline (and not compatible with certain substrates), hydrogen peroxide can be stored and used as a stable 30% neutral aqueous solution, and its only inorganic oxidation byproduct is water, reducing both its transportation costs and waste generation.[7] Therefore, there is a pressing need to develop efficient methods for oxidizing alcohols to carbonyl compounds using hydrogen peroxide.

Shanghai Pinghe School, 333 Shenqi Road, Pudong New District, Shanghai, China. E-mail: michaelhe0319@gmail.com; Tel: +86 150 2123 3875

However, under ambient conditions, hydrogen peroxide, like many renewable oxidants, reacts slowly with most alcohols, necessitating the use of a redox-active catalyst to enhance the reaction rate. Ideally, such a catalyst should combine high activity with environmental sustainability: it should be easily separated and recycled, and toxic or hazardous precursors used in its synthesis should be separated before use in order to minimize waste and environmental impact.[8] This presents significant challenges for the development of alternative catalytic systems.[9] Heterogeneous catalysts offer distinct advantages over their homogeneous counterparts, as they remain insoluble in the reaction medium and can be readily recovered by filtration or centrifugation. When used in bulk form, however, their catalytic activity is limited by the low interfacial surface area. To overcome this limitation, active catalytic components can be dispersed onto inert supports, such as silica, alumina, or activated carbon, significantly enhancing the effective surface area and catalytic performance. This approach forms the basis of many industrial heterogeneous catalysts.[10,11] Transition metals such as palladium, silver, and gold are well-established redox catalysts that facilitate both oxidation and reduction reactions and are thus widely applied in industrial catalysis.[12,13] Therefore, it is reasonable to deduce that these transition metals could also catalyze the oxidation of primary alcohols to carbonyl compounds.

A further challenge lies in the biphasic nature of the reaction system: alcohol substrates typically exhibit poor solubility in water, whereas hydrogen peroxide is aqueous, which reduces the interfacial contact and thereby slows the reaction. One effective strategy to address this issue involves modifying the surface properties of the inert support material, adjusting, for example, its hydrophilicity or hydrophobicity, to promote the formation of stable oil–water emulsions. These so-called Pickering emulsions significantly increase the contact area between phases, thereby enhancing mass transfer and reaction rates.[14] Furthermore, such systems allow the aqueous phase (containing the oxidant) to be encapsulated within droplets suspended

in the organic phase (containing the alcohol substrate), enabling the continuous flow of the organic phase and simultaneous product extraction. This continuous-flow design offers considerable advantages over traditional batch processes by improving scalability, reducing the number of purification steps, and increasing reaction efficiency.[15]

To address the limitations described above, this work presents a novel two-phase oxidation system based on Pickering emulsions stabilized by silica-supported metal nanoparticles. These emulsions can be conveniently packed into a glass column to enable efficient oxidation of primary benzylic alcohols to aldehydes.[14] Specifically, a stable water-in-oil Pickering emulsion is formed by mixing an aqueous hydrogen peroxide solution with an organic solvent and the silica-supported nanoparticles, which act as both catalysts and emulsifiers. The emulsion is then loaded into a column reactor. By continuously introducing the alcohol-containing organic phase into the column, the system enables steady production of aldehydes as the reaction proceeds along the flow path. This approach combines several advantages, including low cost, mild reaction conditions, and full catalyst recyclability.

A key innovation of this system is the use of a chromatography-type glass column as the reactor, which facilitates the simultaneous introduction of substrates and collection of products, realizing a truly continuous-flow process.[15] Furthermore, the unique Pickering emulsion structure ensures uniform catalyst distribution at the oil–water interface, which significantly enhances both the rate and efficiency of the oxidation reaction.

2 Materials and methods

2.1 Materials

The materials used are displayed in Table 1.

2.2 Preparation of dendritic mesoporous silica nanoparticle (DMSN) catalysts

2.2.1 Preparation of unmodified DMSNs (DMSNs-raw). A mixture of 19.2 g of cetyl trimethyl ammonium tosylate (CTATos), 3.47 g of triethanolamine (TEAH3 > 78 wt%), and 1000 mL of deionized water was stirred at 80 °C for 1 h. Next, 145.8 g of tetraethyl orthosilicate (TEOS) was quickly added to the surfactant solution. The mixture was then stirred at 80 °C with a stirring speed of 1200 rpm for another 2 h. Following this, the mixture was centrifuged at 11 000 rpm for 5 min, washed once with ethanol (1000 mL), and dried in an oven at 100 °C. Then, the DMSNs-raw was calcined in air at a heating rate of 2 °C min^{-1} and kept at 550 °C for 6 h to remove the surfactants.

2.2.2 Acid washing of DMSNs-raw. 18 g of DMSNs-raw was suspended in 720 mL of ethanol. 30.24 mL of 1 M HCl was added, and the mixture was refluxed at 60 °C for 2 h. After refluxing, the mixture was centrifuged at 8000 rpm for 2 min and washed with 480 mL of ethanol. The acid-washed DMSNs-raw (DMSNs-acid) was dried at 80 °C.

2.2.3 Hydrophobic surface modification of DMSNs (DMSNs-methyl). 13.5 g DMSNs-acid was dispersed in toluene (72 mL). A mixture of 5.45 g of methyltrimethoxysilane and 4.05 g of triethylamine was then added to the suspension. The resulting mixture was refluxed under an N_2 atmosphere for 4 h, after which it was centrifuged at 8000 rpm for 2 min. The solid was washed four times with 80 mL of toluene per wash and then dried at 110 °C to yield DMSNs-methyl.

2.2.4 Metal loading of hydrophobic DMSNs

2.2.4.1 Silver-modified DMSNs-methyl (DMSNs-Ag). 5 g of DMSNs-methyl was dispersed in 150 mL of ethanol, followed by the addition of 0.1575 g of silver nitrate. The mixture was stirred in the dark for 2 h, after which 0.481 g of sodium borohydride was added in one portion. Stirring was continued for another 30 min under dark conditions. The product was then centrifuged at 8000 rpm for 2 min and washed with 150 mL of acetone. The resulting DMSNs-Ag was dried at 80 °C.

2.2.4.2 Palladium-modified DMSNs-methyl (DMSNs-Pd). In a similar procedure, 0.1656 g of palladium(II) chloride was used in place of silver nitrate. All other experimental conditions remained the same.

2.2.5 Characterization of DMSN catalysts. At each step, the DMSN catalysts were characterized by several techniques.

Table 1 Materials used in the experiments

Reagent	Molecular formula	Purity	Supplier
Tetraethyl orthosilicate	$C_8H_{20}O_4Si$	98%	Macklin
Cetyltrimethylammonium *p*-toluenesulfonate	$C_{26}H_{49}NO_3S$	AR	Macklin
Ethanol	C_2H_6O	99.9%	Titan
Triethanolamine	$C_6H_{15}NO_3$	AR	Aladdin
Hydrochloric acid	HCl	36–38%	Sinopharm
Toluene	C_7H_8	AR	Sinopharm
Triethylamine	$C_6H_{15}N$	99%	Titan
Methyltrimethoxysilane	$C_4H_{12}O_3Si$	98%	Macklin
Sodium borohydride	$NaBH_4$	98%	Adamas
Silver nitrate	$AgNO_3$	99.95–100.05%	Sinopharm
Palladium(II) chloride	$PdCl_2$	98%	Macklin
Acetone	C_3H_6O	AR	Sinopharm
Nile red	$C_{20}H_{18}N_2O_2$	98%	Macklin
Hydrogen peroxide	H_2O_2	30%	Sinopharm
Benzyl alcohol	C_7H_8O	99%	Adamas

Transmission electron microscopy (TEM, Hitachi HT7700 operating at 100 kV) was used to examine the particle morphology and diameter. Energy-dispersive X-ray spectroscopy (EDS), integrated with the TEM, confirmed the elemental composition. XPS analysis was performed with a Thermo Scientific K-Alpha. Nitrogen adsorption–desorption isotherms were recorded using a Micromeritics ASAP 2460 Version 3.01 to determine the surface area to volume ratio. Finally, the hydrophilicity or hydrophobicity of the nanoparticles was assessed by contact angle measurements using a Ding Sheng JY-82C automatic video contact angle instrument. For these measurements, the DMSN powder was compressed into a disc using a mold. Palladium loading levels of DMSNs-Pd were determined by digesting a certain mass of DMSNs-Pd with 0.2 mL reverse aqua regia (68% HNO_3 : 37% HCl = 3 : 1 v/v), sonicating for 10 min, adding deionized water to 10 mL volume, filtering through a 0.22 μm filter membrane, and measuring the Pd concentration of the resulting solution by ICP-MS.

2.3 Preparation and characterization of the Pickering emulsion system

2.3.1 General preparation of Pickering emulsions. A mixture of 2 mL of toluene (or a solution of benzyl alcohol in toluene), a defined mass of a type of DMSNs (1–5% w/v of oil and water phases), and 3 mL of water (or hydrogen peroxide aqueous solution) in a 15 mL centrifuge tube was mixed on a VORTEX-6 Vortex Mixer (Haimen Kylin-Bell Lab Instruments Co., Ltd) at room temperature and 2800 rpm until the mixture became macroscopically uniform and opaque (around 2 min).

2.3.2 Characterization of the Pickering emulsions. To visualize the oil phase, a small amount of Nile red was dissolved in toluene. A mixture of dyed toluene (2 mL), DMSNs-methyl (0.05, 0.15, or 0.25 g), and water (3 mL) was shaken by hand until the mixture became macroscopically uniform and opaque. Fluorescence confocal microscopy images of the resulting Pickering emulsions were taken using an Olympus FV3000 confocal laser scanning microscope. The stability of the emulsion was tested by taking fluorescence confocal microscopy images after allowing the mixture with 0.05 g DMSNs-methyl to stand for 3, 6, 9 and 12 hours.

2.3.3 Comparison of batch and Pickering emulsion reactions. 6 mL of 6% hydrogen peroxide aqueous solution (prepared by mixing 30% hydrogen peroxide and deionized water in 1 : 4 v/v ratio) and 4 mL of 25% benzyl alcohol solution in toluene (prepared by mixing benzyl alcohol and toluene in 1 : 3 v/v ratio) were added into four 20 mL glass vials labeled as vial 1, 2, 3, and 4, with each equipped with a magnetic stir bar. Then 0.16 g (1.33% w/v) of DMSNs-methyl was added to vial 2, 0.16 g of DMSNs-Pd was added to vial 3, and 0.16 g of DMSNs-Ag was added to vial 4, while no DMSNs were added to vial 1. The three vials containing DMSNs were shaken by hand until the mixture became macroscopically uniform and opaque. After emulsification, the four vials were stirred at 2000 rpm at room temperature. Samples were taken at intervals and analyzed by HPLC (Thermo Fisher Scientific UltiMate 3000) to determine the conversion.

2.3.3.1 Sampling method. 20 μL of organic phase was taken from a vial and diluted with 1980 μL of acetonitrile in a 2 mL centrifuge tube to create a solution of the sample (100 times dilution) in acetonitrile. The sample was analyzed by HPLC (Thermo Fisher Scientific UltiMate 3000).

2.3.4 Investigation of catalyst load in the oxidation reaction. After adding 6 mL of 6% hydrogen peroxide aqueous solution and 4 mL of 25% benzyl alcohol solution in toluene into three 20 mL glass vials labeled vials 1, 2, and 3, each of which was equipped with a magnetic stir bar, and adding 0.1 g (1% w/v) of DMSNs-Pd to vial 1, 0.3 g (3% w/v) of DMSNs-Pd to vial 2, and 0.5 g (5% w/v) of DMSNs Pd to vial 3, the three vials were shaken by hand until the mixture became macroscopically uniform and opaque. After emulsification, the vials were stirred at 2000 rpm at room temperature. Samples were taken at intervals (15 min, 30 min, 45 min, 1 h, 2 h, 3 h, 4 h, 6 h, 12 h) and analyzed by HPLC (Thermo Fisher Scientific UltiMate 3000) to determine the conversion.

2.3.4.1 Sampling method. 20 μL of organic phase was taken from a vial and diluted with 380 μL of toluene in a 1 mL centrifuge tube. The tube was centrifuged at 8000 rpm for 2 min. 200 μL of the supernatant was taken from the tube and diluted with 800 μL of acetonitrile in another centrifuge tube to create a solution of the sample (100 times dilution) in acetonitrile. The sample was analyzed by HPLC (Thermo Fisher Scientific UltiMate 3000).

2.4 Assembly and tests of the column reactor

2.4.1 General assembly of the column reactor. A glass column fitted with a glass frit at its base (8 mm in diameter and a sand filter with a pore diameter of 10 μm) was used as the reactor. A given volume of Pickering emulsion was poured into this column, forming a packed bed. The continuous oil phase (toluene/benzyl alcohol) was added at once from the top of the column, and the eluent was collected from the outlet of the column. The flow rate was determined based on the volume of the collected liquid per unit of time.

2.4.2 Alcohol oxidation reaction using the column reactor. A Pickering emulsion formulated with 10 mL of 6% aqueous hydrogen peroxide, 6 mL of toluene, 0.16 g of DMSNs-Pd (1% w/v), and 0.32 g of DMSNs-methyl (2% w/v) was used to assemble a column reactor. Then, 5 mL of 25% benzyl alcohol solution in toluene was added at once from the top of the column. Samples of the eluent were taken at intervals and analyzed by HPLC to determine the conversion.

2.4.2.1 Sampling method. A 2 mL centrifuge tube was used to collect the eluent of the column in a certain timeframe. The volume of the eluent was measured using a pipette. The eluent was diluted with acetonitrile to create a solution of the sample (100 times dilution). The sample was analyzed by HPLC (Thermo Fisher Scientific UltiMate 3000).

3 Results and discussion

3.1 Synthesis and characterization of DMSNs

Dendritic silica mesoporous nanoparticles (DMSNs) were synthesized *via* a sol–gel process described in the literature.

Briefly, tetraethyl orthosilicate (TEOS) was hydrolyzed in the presence of a cationic surfactant and an organic base. Following hydrolysis, the particles were separated by centrifugation and calcined to remove the surfactant.[14] The as-synthesized DMSNs were then washed with acid to further remove the remaining traces of the organic base, preparing the silica surface for subsequent modification with methyltrimethoxysilane. This modification introduced methyl groups into the silica framework, imparting hydrophobic properties to the nanoparticles. Finally, transition-metal nanoparticles were deposited on the hydrophobic modified DMSNs by reducing the corresponding metal salts with sodium borohydride in alcoholic solution.

Post-synthesis, the DMSNs catalysts were characterized using TEM, EDS, and contact angle measurements. As shown in Fig. 1, the average diameter of all five types of DMSNs was consistent at around 210 nm, roughly twice the size reported in previous studies, which may be attributed to insufficient stirring and heat supply during synthesis.[16] The particles generally exhibited a distinctive dendritic morphology consistent with literature reports, confirming the successful synthesis of the DMSNs. Notably, some particles displayed relatively smooth surfaces with no visible dendritic features, which is likely due to local variations in concentration and temperature during the reaction.

After confirming the presence of palladium in DMSNs-Pd by EDX, further analysis with XPS revealed the valence state of Pd in the nanoparticles. As seen in Fig. 2, peaks corresponding to oxygen, carbon and palladium are present. A magnified view of the Pd 3d peak is shown in Fig. 2(d), and the two peaks shown in red at 335 and 340 eV match with the known XPS spectrum of palladium metal, while the two (smaller) peaks shown in green at 337 and 343 eV match that of palladium(II) oxide, indicating that palladium exists in DMSNs-Pd as both Pd(0) and, to a less extent, Pd(II). The palladium loading of DMSNs-Pd was determined to be 1.410 wt% *via* ICP-MS.

To verify the successful loading of transition metals onto the DMSNs, energy-dispersive spectra (EDS) were collected for all five types of DMSNs. All EDS scans consistently revealed a homogeneous distribution of silicon and oxygen throughout the samples, as illustrated in Fig. 3 and 4. Importantly, the weight percentages of silicon and oxygen remained essentially unchanged between DMSNs-raw and DMSNs-methyl, indicating that the hydrophobic surface modification did not alter the elemental composition of the silica substrate. In the two

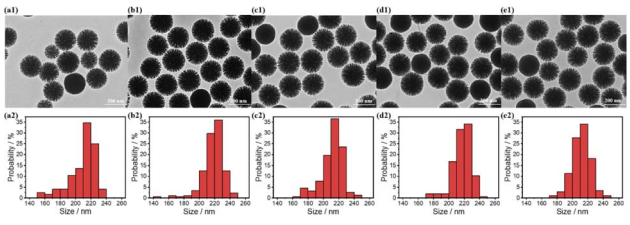

Fig. 1 (a1–e1) TEM images and (a2–e2) size distribution histograms of (a) DMSNs-raw, (b) DMSNs-acid, (c) DMSNs-methyl, (d) DMSNs-Ag, and (e) DMSNs-Pd.

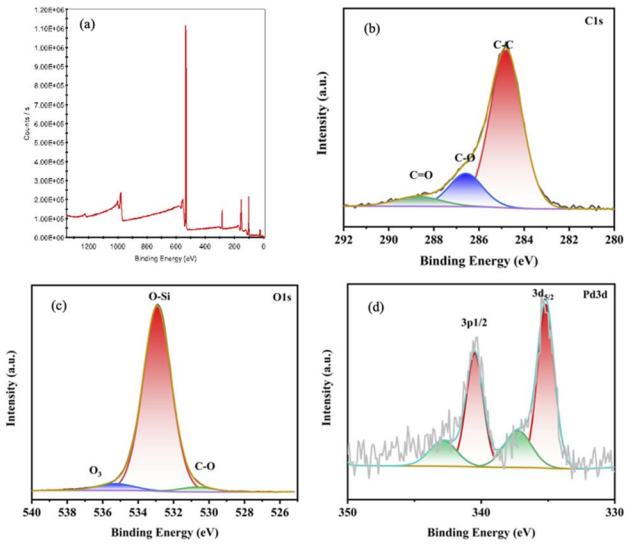

Fig. 2 (a) Full XPS spectrum and (b) C 1s, (c) O 1s, and (d) Pd 3d spectra of DMSNs-Pd.

samples of DMSNs loaded with metals shown in Fig. 4, the metal signals were found to be located on the silica nanospheres, indicating that the metal loading step was successful.

The BET surface areas of the DMSNs, as well as their pore size distribution, were obtained from nitrogen absorption–desorption isotherms. As shown in Fig. 5(a)–(e), the large BET surface area of all the DMSNs highlights their potential use as catalyst supports. The BET surface area of the DMSNs decreases after both acid wash and hydrophobic modification, but only changes slightly with metal loading. The pore diameter of the DMSNs is fairly consistent during the steps, as displayed by the cumulative curves, and the pore diameter distribution peaks at 20 nm, reflecting the mesoporous nature of the DMSNs.

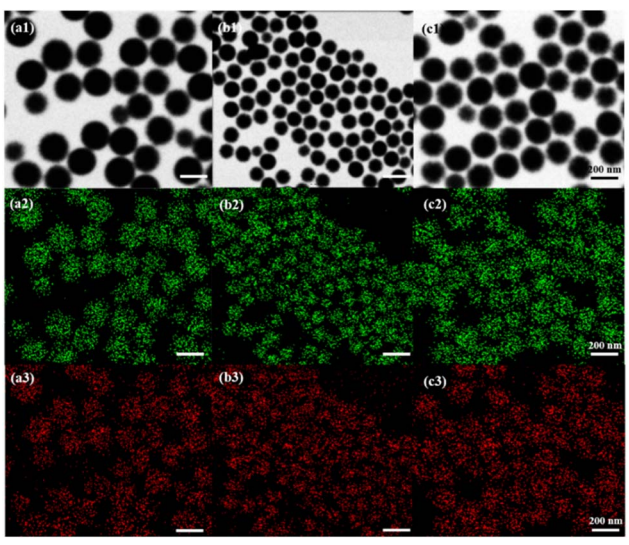

Fig. 3 (a1–c1) TEM images of nanoparticles; (a2–c2) EDS scans of Si $K\alpha_1$; (a3–c3) EDS scans of O $K\alpha_1$ for (a) DMSNs-raw, (b) DMSNs-acid, and (c) DMSNs-methyl.

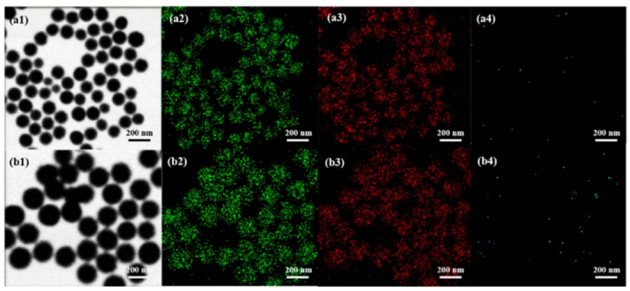

Fig. 4 (a1 and b1) TEM images of nanoparticles; (a2 and b2) EDS scans of Si Kα_1; (a3 and b3) EDS scans of O Kα_1; and (a4 and b4) EDS scans of Ag (or Pd) Lα_1 for (a) DMSNs-Ag and (b) DMSNs-Pd.

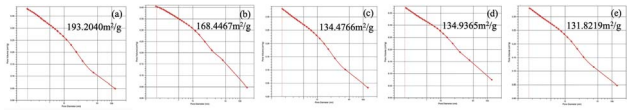

Fig. 5 (a–e) Nitrogen absorption–desorption isotherm curves of (a) DMSNs-raw, (b) DMSNs-acid, (c) DMSNs-methyl, (d) DMSNs-Pd and (e) DMSNs-Ag, with their respective BET surface area.

After preparing all the DMSNs, their amphiphilicity was determined *via* contact angle measurements to establish whether they could be used as emulsifiers in the preparation of water-in-oil Pickering emulsions. As shown in Fig. 6(a), the DMSNs-acid exhibited a low contact angle of 21.4°, reflecting the high density of hydrophilic hydroxyl groups. The contact angle increased significantly to 81.3° with DMSNs-methyl (Fig. 6(b)). Further incorporation of metals enhanced the hydrophobicity of the nanoparticles, with contact angles of 85.4° and 98.3° recorded for DMSNs-Ag and DMSNs-Pd, respectively (Fig. 6(c) and (d)). The relatively hydrophobic nature of DMSNs-methyl, DMSNs-Ag, and DMSNs-Pd renders them effective emulsifiers for stabilizing water-in-oil interfaces in Pickering emulsions.

3.2 Preparation and characterization of the Pickering emulsion system

Having prepared these hydrophobically modified nanoparticles, their ability to form water-in-oil Pickering emulsions was evaluated. In one example, DMSNs-methyl was employed to prepare the emulsion. A mixture comprising 3.33 mL of water, 1.66 mL of toluene dyed with Nile red (0.014 g L^{-1}), and 0.05 g of DMSNs-methyl (corresponding to 1% w/v of the emulsion) was shaken by hand until a macroscopically uniform, opaque emulsion was achieved. Fluorescence confocal microscopy analysis (Fig. 7(a)) revealed colorless droplets dispersed within a red continuous phase, thereby confirming that nanoparticles assembled at droplet interfaces to form micron-sized emulsions, where the oil phase is continuous and the water phase is dispersed in oil. When the concentration of DMSNs-methyl was increased to 3% and 5% w/v, the water droplet size decreased, as more nanoparticles were available to stabilize the increased interfacial area (Fig. 7(b) and (c)).

This variation in droplet size facilitated the investigation of the influence of both catalyst concentration and droplet size on the catalytic efficiency. The long-term stability of the emulsion (up to 12 hours) was confirmed by the consistent size of the water droplets after standing (Fig. 8(a)–(e)).

Following the successful formation of water-in-oil Pickering emulsions, the catalytic activity of the DMSNs in these systems was examined for the oxidation of benzyl alcohol. Benzyl alcohol was chosen as the model substrate due to its accessibility and ease of analysis. Four types of batch reaction systems (Fig. 9) were designed to compare the catalytic efficiency of the Pickering emulsions stabilized with different nanoparticle catalysts:

System 1: a batch reaction without any DMSNs, where benzyl alcohol was dissolved in a water-immiscible solvent (toluene) and mixed with an aqueous solution of hydrogen peroxide.

System 2: a batch reaction with Pickering emulsions stabilized by 1.33% w/v DMSNs-methyl.

System 3: a batch reaction using Pickering emulsions stabilized by 1.33% w/v DMSNs-Pd.

System 4: a batch reaction using Pickering emulsions stabilized by 1.33% w/v DMSNs-Ag.

Each system was magnetically stirred at room temperature, and aliquots were periodically withdrawn for analysis *via* HPLC (Thermo Fisher Scientific UltiMate 3000).

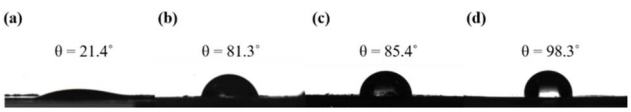

Fig. 6 (a–d) Contact angle measurement results of (a) DMSNs-acid, (b) DMSNs-methyl, (c) DMSNs-Ag, and (d) DMSNs-Pd.

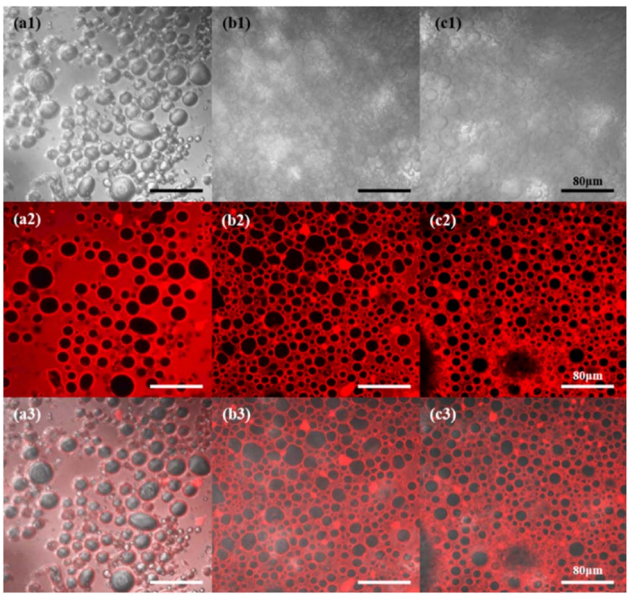

Fig. 7 (a–c) Fluorescence confocal microscopy images of the micron-sized Pickering emulsions formulated with different amounts of DMSNs-methyl nanoparticles: (a) 1%, (b) 3%, and (c) 5%. These images were taken in different fields: (1) bright, (2) Nile red, and (3) merge.

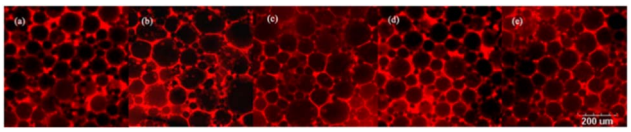

Fig. 8 (a–e) Fluorescence confocal microscope images of the Pickering emulsions formed from DMSNs-methyl (a) 0, (b) 3, (c) 6, (d) 9, and (e) 12 hours after preparation.

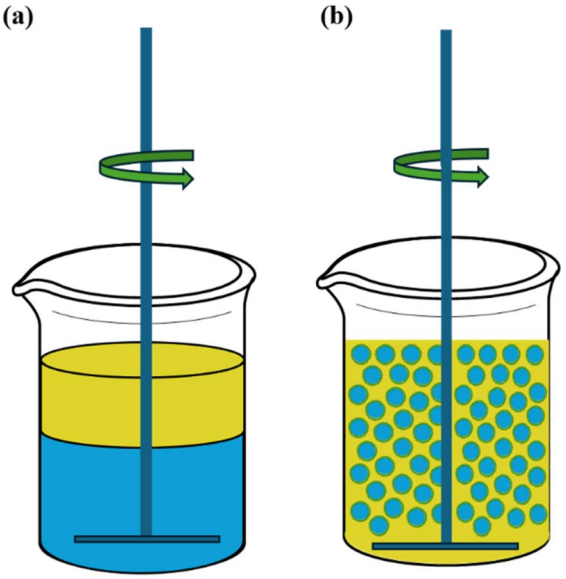

Fig. 9 Schematic of the design of system 1 (a) and systems 2, 3, and 4 (b). In the systems with Pickering emulsions, the water layer (blue) is compartmentalized into droplets within the oil phase (yellow).

A typical HPLC chromatogram (Fig. 10) exhibits sharp peaks at 4.75, 7.03, and 8.07 min, corresponding to benzyl alcohol, benzaldehyde, and benzoic acid, respectively. A broad peak centered at 12.63 min, attributable to an unidentified substance under investigation, was not considered in the conversion calculations. The relative concentration of each component was determined based on the area under its corresponding peak.

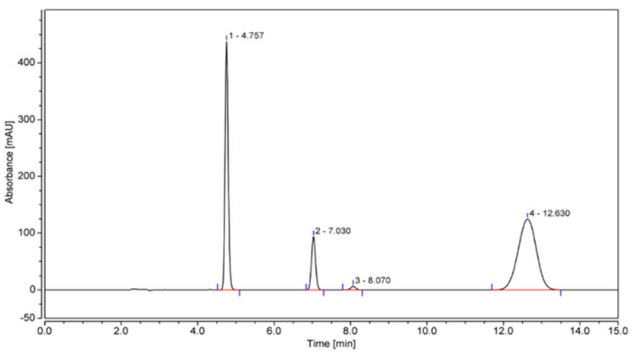

Fig. 10 A typical HPLC analysis curve shows four distinctive peaks: benzyl alcohol (1), benzoic acid (2), benzaldehyde (3), and an unknown substance (4).

Given that the oxidation of benzyl alcohol to benzaldehyde by hydrogen peroxide is a heterogeneous (biphasic) reaction, efficient conversion was not expected in system 1 due to the absence of a catalyst and insufficient contact between the phases (Fig. 11(a)). As shown in Fig. 11(a), the percentage of unreacted benzyl alcohol ranged from 77% after 0.5 h to 92% after 23 h. The conversion of alcohol into the aldehyde and acid did not exceed 22%, consistent with expectations. Similarly, system 2, which contained only DMSNs-methyl, exhibited negligible benzaldehyde formation, although the concentrations of benzoic acid and unreacted benzyl alcohol varied significantly: benzoic acid initially reached 45% conversion and then decreased over time, while the percentage of residual benzyl alcohol increased from 55% to 95% (Fig. 11(b)).

In contrast, system 3, employing DMSNs-Pd, demonstrated remarkable performance. Benzaldehyde conversion rapidly increased to 94% within 1 h and remained above 80% throughout the experiment, while the levels of benzyl alcohol and benzoic acid stayed below 15% (Fig. 11(c)). Conversely, system 4, containing DMSNs-Ag, exhibited trends similar to that of system 2: the concentrations of benzyl alcohol and benzoic acid were initially comparable (58% *vs.* 41%), with benzoic acid decreasing to 0% by 23 h and benzaldehyde remaining nearly undetectable (Fig. 11(d)).

Overall, DMSNs-Pd proved to be the superior catalyst for the selective oxidation of benzyl alcohol to benzaldehyde, achieving rapid conversion with minimal formation of side products such as benzoic acid, whereas the other catalysts failed to produce high conversions (Fig. 12). The catalytic effect of DMSNs-Pd was substantiated by repeating the procedure in triplicate (Fig. 13). The activity of DMSNs-Pd based on Pd content was calculated as 10.2 mol g_{Pd}^{-1} h^{-1}, from the previously obtained 1.410 wt% Pd loading and the 74.8% area of benzaldehyde after 0.5 h of reaction.

With the standard conditions established, experiments using higher hydrogen peroxide concentrations were performed

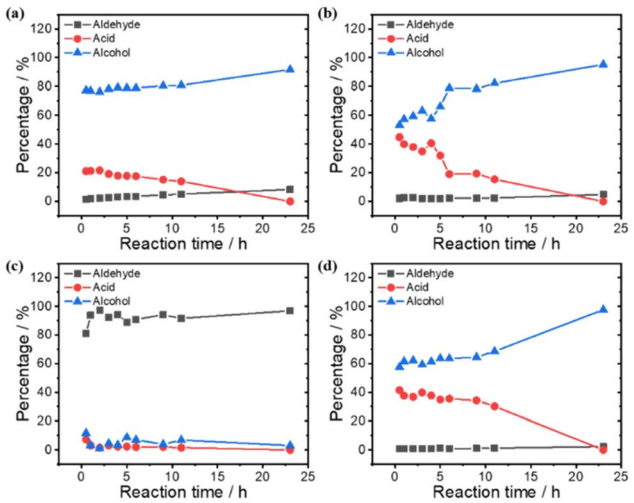

Fig. 11 Percentage of the products (aldehyde and acid) or percentage of the remaining substrate (alcohol) of (a) system 1, (b) system 2, (c) system 3, and (d) system 4.

to optimize the conversion. However, as seen in Fig. 14, increasing the concentration of hydrogen peroxide from 6% to 12% did not increase the conversion or the selectivity of benzaldehyde. During the experiment, it was observed that large amounts of oxygen gas evolved when the mixture was emulsified, suggesting that the higher concentration of hydrogen peroxide is susceptible to catalytic decomposition by DMSNs-Pd before it can participate in the oxidation reaction. Hence, 1 molar equivalent of 6% hydrogen peroxide appears to be a well-rounded choice to lower cost and minimize unwanted decomposition.

The choice of oxidant was then switched to 12% sodium hypochlorite, another common reagent in green oxidation of alcohols, to determine which is superior and to elucidate the reaction mechanism. From Fig. 15, it is seen that the conversion of benzyl alcohol into benzaldehyde was only around 70%, considerably lower than that with hydrogen peroxide, while the amount of benzoic acid produced was much higher. Thus, DMSNs-Pd is better used with hydrogen peroxide instead of sodium hypochlorite in this catalytic oxidation procedure. The decomposition of sodium hypochlorite is catalyzed by numerous transition-metal ions, but not palladium,[17] while hydrogen peroxide evolves significant quantities of oxygen gas when in contact with DMSNs-Pd. Oxygen thus seems to be essential for the oxidation of benzyl alcohol to benzaldehyde, and may be a critical step in the mechanism, as discussed below.

The heterogeneous catalytic effect of DMSNs-Pd was further confirmed by centrifuging the reaction mixture (same composition as system 3) after 15 min to remove the catalyst and monitoring the reaction for 24 h. As seen in Fig. 16, no substantial changes in the reactant or product concentration are seen when the catalyst is removed, proving true heterogeneous catalysis.

Following the demonstration of high catalytic activity for DMSNs-Pd in the selective oxidation of benzyl alcohol, the effect of its concentration on oxidation efficiency was further investigated. Parallel experiments were conducted in three 20 mL vials, each containing identical amounts of benzyl alcohol, toluene, and hydrogen peroxide solution, with the DMSNs-Pd catalyst added at 1%, 3%, and 5% w/v, respectively. After emulsification by sonication, aliquot samples were periodically withdrawn and analyzed by HPLC using an improved sampling method, involving dilution with toluene, centrifugation, and subsequent dilution of the supernatant with acetonitrile, to prevent further catalysis during the sampling process. All three systems showed decently high conversion and selectivity towards benzaldehyde, with conversion reaching as high as 88% at 12 h for 5% w/v DMSNs-Pd and no obvious formation of benzoic acid over the entire reaction span of 12 h (Fig. 17). For each system, a slight improvement in percentage conversion was observed when the catalyst load was increased from 1% to 5% w/v, *e.g.*, from 79% at 15 min to 88% at 12 h for 5% w/v DMSNs-Pd. Also, notably, the percentage conversion increased only slightly as the catalyst load increased; for example, from 79% for 1% w/v DMSNs-Pd to 84% for 3% w/v and 88% for 5% w/v DMSNs-Pd at 12 h. As the decreasing activity (8.05, 3.55 and 2.05 mol g_{Pd}^{-1} h^{-1} for 1%, 3% and 5% w/v, respectively) shows, the efficiency-limiting variable is not the number of palladium sites. Instead, the only slight decrease in droplet size of the emulsion (and thus the increase in interfacial area) when the catalyst load is increased, as observed above in the emulsion characterization, may explain why the increase in conversion is small when catalyst loading is increased. Therefore, 1% w/v DMSNs-Pd was selected as the optimal catalyst load in terms of better economy and fewer other side reactions (*e.g.*, the degradation of hydrogen peroxide under the catalysis of Pd nanoparticles).

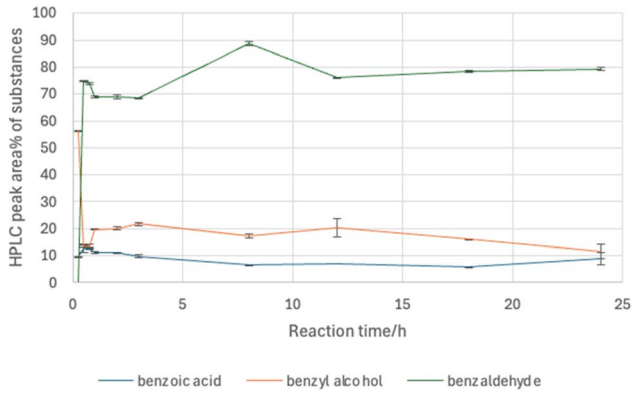

Fig. 13 Results of the triplicate repetition of the standard batch Pd reaction (system 3).

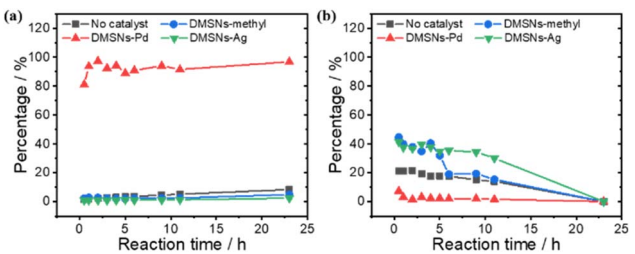

Fig. 12 Comparison of the percentage of (a) aldehyde and (b) acid in different systems.

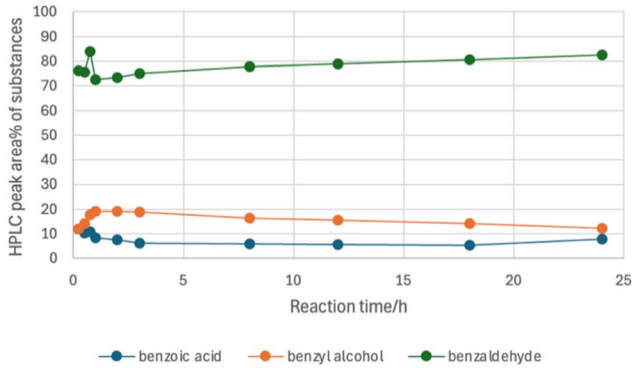

Fig. 14 Percentage of the products and substrate with 12% hydrogen peroxide.

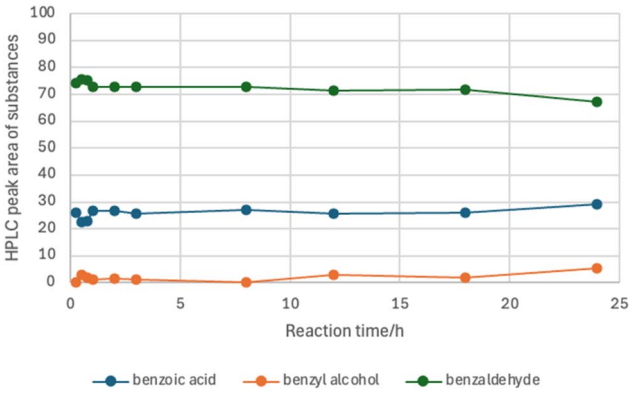

Fig. 15 Percentage of products and substrate produced with 12% sodium hypochlorite.

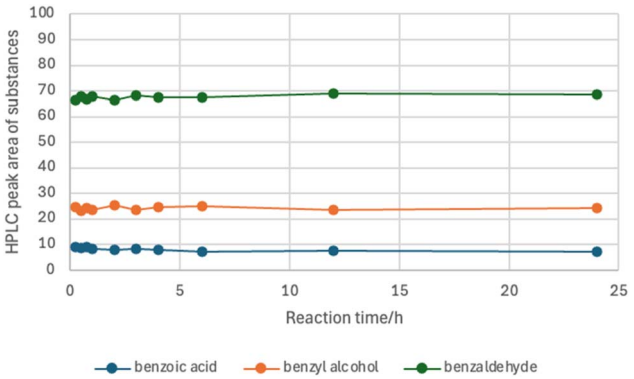

Fig. 16 Percentage of products and substrate formed with the catalyst removed.

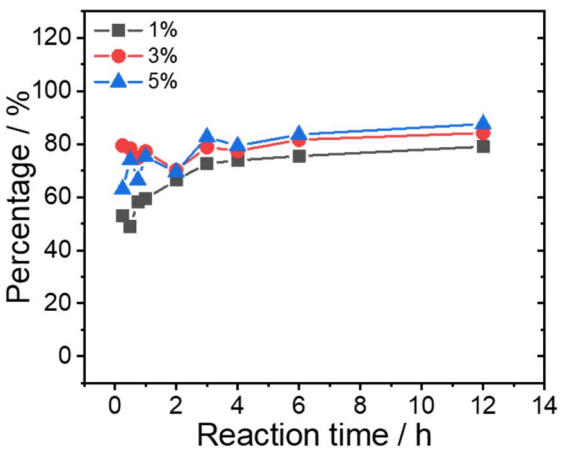

Fig. 17 Comparison of the percentage conversion of aldehyde in the systems with different amounts of DMSNs-Pd.

A brief discussion of the postulated reaction mechanism is presented here. The selective alcohol oxidation reaction is most likely to be achieved *via* a catalyst/reagent with an intermediate oxidation potential that is able to oxidize alcohol to aldehyde but not further. Interestingly, previously reported catalysts/reagents of alcohol oxidation with hydrogen peroxide, such as magnetite and nitric acid,[18–20] have standard electrode potentials similar to that of palladium (Fe_3O_4–Fe(II) = 0.98 V, HNO_3–HNO_2 = 0.94 V, Pd(II)–Pd = 0.915 V), so a redox pair with standard electrode potential in this margin of 0.9–1.0 V has the potential to catalyze this reaction. To explain the microscopic steps of the reaction, mechanisms in previous literature were investigated. Based on previous work on the oxidation of benzyl alcohol with gold catalysts,[21] the adsorption of hydrogen peroxide and benzyl alcohol molecules was followed by the surface reaction between them and the desorption of the benzaldehyde product. A more detailed view of the possible surface reactions is seen in another work discussing the oxidation of benzyl alcohol with molecular oxygen, where oxygen atoms adsorbed on palladium abstract hydrogen atoms from benzyl alcohol, forming benzaldehyde and two hydroxyl radicals that recombine to form hydrogen peroxide.[22] As hydrogen peroxide is catalytically decomposed to oxygen, as seen in the experiments, it is postulated that the primary oxidant in the reaction is molecular oxygen adsorbed on the Pd surface, formed by the decomposition of hydrogen peroxide in the water phase. As the solubility of nonpolar molecular oxygen is higher in toluene than in water, it immediately dissolves in the oil phase and is consumed in the oxidation of benzyl alcohol. This *in situ* production and immediate consumption of oxygen may explain the superior selectivity of benzaldehyde and minimal production of benzoic acid in the oxidation system. The unique catalytic activity of palladium in comparison to other noble metals with similar chemical and catalytic properties (gold, silver, and especially platinum) could also be explained by its propensity to adsorb large amounts of small molecules on its surface. Of course, this proposed mechanism still needs to be supported by more observations and evidence.

3.3 Construction of a column reactor for continuous-flow oxidation

Based on the promising performance of 1% w/v DMSNs-Pd in the batch reactions, a continuous-flow reactor was subsequently constructed. The reactor consists of a glass column of around 1 cm in diameter with a fritted sand filter at the bottom. As illustrated by the schematics in Fig. 18(a), the catalyst-containing Pickering emulsion is loaded into the column, and the benzyl alcohol substrate is added from the top. Due to the configuration, *i.e.*, the water droplet diameters of 15–20 μm exceed the bore diameter of the frit, the droplets are retained within the column while the oil phase flows through.

The alcohol oxidation reaction was performed using this setup with an emulsion prepared with 10 mL of 6% hydrogen peroxide, 6 mL of toluene, and defined amounts of emulsifier. According to the procedure in Section 2.3.1, 1% w/v DMSNs-Pd was employed as the active catalyst, while 2% w/v DMSNs-methyl was used as an additional emulsifier to strengthen the emulsion, making it sufficiently stable for use in the column reactor. Around 5 mL of 25% benzyl alcohol solution in toluene was then added from the top of the column, and the oil phase was allowed to elute off the column without applied pressure. Eluted samples were collected at various time points and analyzed by HPLC.

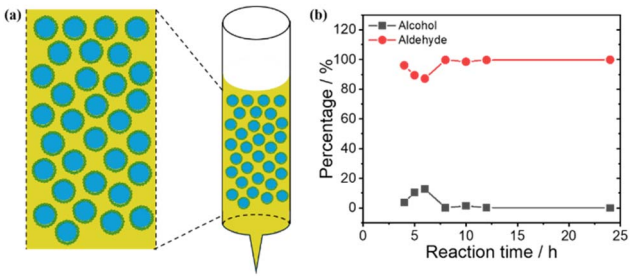

Fig. 18 (a) Schematic of the continuous-flow column reactor containing compartmentalized water spheres (blue) surrounded by nanoparticles (green) suspended in the oil phase (yellow). (b) Percentage of the produced aldehyde and percentage of the remaining alcohol in the column reaction.

As shown in Fig. 18(b), during the first 3 h, benzaldehyde was undetectable, and only a small amount of benzyl alcohol was present, which can be attributed to the exchange of the initial loading solvent. Beginning at the fourth hour, a substantial concentration of benzaldehyde appeared in the eluent, and its concentration remained above 90% for the remainder of the 24 hour run, with no detectable benzoic acid formed. Therefore, the column reactor continuously converted benzyl alcohol into benzaldehyde in near-quantitative yield over reasonable periods, which makes the system applicable in actual laboratory preparation of aldehydes from alcohols.

4 Conclusion

In this study, a novel silica-supported transition-metal nanoparticle catalyst was prepared, characterized, and evaluated as an efficient and selective system for the oxidation of benzylic alcohols to aldehydes using hydrogen peroxide. The mesoporous silica substrate was synthesized *via* a modified sol–gel method, subsequently surface-modified with hydrophobic groups, and finally loaded with transition-metal nanoparticles, yielding a DMSNs-metal composite catalyst. This catalyst was employed in the preparation of Pickering emulsions, and its catalytic performance was assessed in both batch and column reactor systems. Notably, the DMSNs-Pd catalyst exhibited the most outstanding performance toward the model substrate benzyl alcohol, consistently achieving near-quantitative conversion to the corresponding aldehyde under all tested reaction conditions. To the best of our knowledge, this is the first report on the use of Pickering emulsion systems for the oxidation of alcohols. Importantly, the reaction system achieves a selectivity towards benzyl alcohol of over 90% and generates no byproducts other than water and minimal (<10%) amounts of benzoic acid, thereby aligning with the principles of green chemistry. This environmentally benign approach demonstrates significant potential for further scale-up in industrial applications.

Conflicts of interest

There are no conflicts to declare.

Data availability

All experimental data supporting this study, including raw characterization data (*e.g.*, TEM and XRD), HPLC yield calculations, microreactor design parameters, and additional details can be obtained from the corresponding author upon reasonable request.

Acknowledgements

I would like to thank Dr Kun Zhang from the Shanghai Key Laboratory of Green Chemistry and Chemical Processes of East China Normal University for his invaluable, free-of-charge guidance throughout the research process (China Youth Talent Program), particularly in selecting the research topic, conducting experiments, and refining this paper. After my decision to investigate liquid-phase oxidation, Dr Zhang suggested designing a continuous-flow system suitable for industrial scenarios, which I took into my design of assembling a Pickering emulsion system in a column for continuous-flow oxidation. I also want to thank the graduate students in Dr Zhang's research group for their guidance in the synthesis of DMSNs, as well as for helping me perform TEM and EDS characterizations. Since Dr Zhang's laboratory does not have access to certain instruments, such as a contact angle measuring instrument, a fluorescence confocal microscope, or HPLC, these experiments were performed at the Suzhou Institute of Nano-Tech and Nano-Bionics (SINANO). I thank Dr Mingsheng Xu at SINANO for guiding and supervising me during the characterizations and HPLC experiments, and during the first draft stage and the revision stage based on peer-review suggestions from *RSC Advances* editors.

References

1 Z. Shariatinia and Z. Karimzadeh, Recent Advances on Oxidation of Alcohols over Various Types of Materials as Effective Catalysts: An Overview, *Coord. Chem. Rev.*, 2025, **526**, 216372, DOI: 10.1016/j.ccr.2024.216372.
2 R. A. Sheldon, Catalytic Oxidations in a Bio-Based Economy, *Front. Chem.*, 2020, **8**, 132, DOI: 10.3389/fchem.2020.00132.
3 J. C. Collins and W. W. Hess, Aldehydes from Primary Alcohols by Oxidation with Chromium Trioxide: Heptanal, *Org. Synth.*, 1972, **52**(5), DOI: 10.15227/orgsyn.052.0005.
4 D. B. Dess and J. C. Martin, Readily Accessible 12-I-5 Oxidant for the Conversion of Primary and Secondary Alcohols to Aldehydes and Ketones, *J. Org. Chem.*, 1983, **48**(22), 4155–4156, DOI: 10.1021/jo00170a070.
5 A. J. Mancuso, S.-L. Huang and D. Swern, Oxidation of Long-Chain and Related Alcohols to Carbonyls by Dimethyl Sulfoxide "Activated" by Oxalyl Chloride, *J. Org. Chem.*, 1978, **43**(12), 2480–2482, DOI: 10.1021/jo00406a041.
6 S. Ma, J. Liu, S. Li, B. Chen, J. Cheng, J. Kuang, Y. Liu, B. Wan, Y. Wang, J. Ye, Q. Yu, W. Yuan and S. Yu, Development of a General and Practical Iron Nitrate/TEMPO-Catalyzed Aerobic Oxidation of Alcohols to Aldehydes/Ketones:

Catalysis with Table Salt, *Adv. Synth. Catal.*, 2011, **353**(6), 1005–1017, DOI: **10.1002/adsc.201100033**.

7 P. Dussault, Applications of Hydrogen Peroxide and Derivatives By C. W. Jones (Formerly of Solvay Interox R&D, Widnes, UK). Royal Society of Chemistry: Cambridge. 1999. X + 264 Pp. £59.50. ISBN 0-85404-536-8, *J. Am. Chem. Soc.*, 2000, **122**(26), 6339–6340, DOI: **10.1021/ja995804x**.

8 *New Beer in an Old Bottle: Eduard Buchner and the Growth of Biochemical Knowledge*, ed. A. Cornish-Bowden, Col·lecció Oberta, Universitat de València, 1997.

9 P. T. Anastas and J. C. Warner, *Green Chemistry: Theory and Practice*, Oxford University Press, Oxford [England], New York, 1998.

10 Z. Ma and F. Zaera, Heterogeneous Catalysis by Metals, in *Encyclopedia of Inorganic Chemistry*, ed. R. B. King, R. H. Crabtree, C. M. Lukehart, D. A. Atwood and R. A. Scott, Wiley, 2005, DOI: **10.1002/0470862106.ia084**.

11 G. Rothenberg, *Catalysis: Concepts and Green Applications*, Wiley-VCH, Weinheim, 2008.

12 T. Li, F. Liu, Y. Tang, L. Li, S. Miao, Y. Su, J. Zhang, J. Huang, H. Sun, M. Haruta, A. Wang, B. Qiao, J. Li and T. Zhang, Maximizing the Number of Interfacial Sites in Single-Atom Catalysts for the Highly Selective, Solvent-Free Oxidation of Primary Alcohols, *Angew. Chem., Int. Ed.*, 2018, **57**(26), 7795–7799, DOI: **10.1002/anie.201803272**.

13 T.-Q. Yang, T.-Y. Ning, B. Peng, B.-Q. Shan, Y.-X. Zong, P. Hao, E.-H. Yuan, Q.-M. Chen and K. Zhang, Interfacial Electron Transfer Promotes Photo-Catalytic Reduction of 4-Nitrophenol by Au/Ag 2 O Nanoparticles Confined in Dendritic Mesoporous Silica Nanospheres, *Catal. Sci. Technol.*, 2019, **9**(20), 5786–5792, DOI: **10.1039/C9CY00967A**.

14 L.-X. Zheng, B. Peng, J.-F. Zhou, B.-Q. Shan, Q.-S. Xue and K. Zhang, High Efficient and Stable Thiol-Modified Dendritic Mesoporous Silica Nanospheres Supported Gold Catalysts for Gas-Phase Selective Oxidation of Benzyl Alcohol with Ultra-Long Lifetime, *Microporous Mesoporous Mater.*, 2022, **342**, 112140, DOI: **10.1016/j.micromeso.2022.112140**.

15 M. Zhang, L. Wei, H. Chen, Z. Du, B. P. Binks and H. Yang, Compartmentalized Droplets for Continuous Flow Liquid–Liquid Interface Catalysis, *J. Am. Chem. Soc.*, 2016, **138**(32), 10173–10183, DOI: **10.1021/jacs.6b04265**.

16 K. Zhang, L.-L. Xu, J.-G. Jiang, N. Calin, K.-F. Lam, S.-J. Zhang, H.-H. Wu, G.-D. Wu, B. Albela, L. Bonneviot and P. Wu, Facile Large-Scale Synthesis of Monodisperse Mesoporous Silica Nanospheres with Tunable Pore Structure, *J. Am. Chem. Soc.*, 2013, **135**(7), 2427–2430, DOI: **10.1021/ja3116873**.

17 E. Živalj, B. Belec and M. Valant, Selective Room-Temperature Catalytic Decomposition of Hypochlorite to Oxygen and Chloride, *ACS Omega*, 2025, **10**(27), 29143–29153, DOI: **10.1021/acsomega.5c01711**.

18 V. A. Matsura, V. V. Potekhin and V. B. Ukraintsev, Kinetics of Hydrogenation and Oxidation of Benzyl Alcohol in the Presence of Colloid Palladium in Situ, *Russ. J. Gen. Chem.*, 2002, **72**(1), 105–109, DOI: **10.1023/A:1015309815764**.

19 S. R. Joshi, K. L. Kataria, S. B. Sawant and J. B. Joshi, Kinetics of Oxidation of Benzyl Alcohol with Dilute Nitric Acid, *Ind. Eng. Chem. Res.*, 2005, **44**(2), 325–333, DOI: **10.1021/ie0303911**.

20 F. Sadri, A. Ramazani, A. Massoudi, M. Khoobi, R. Tarasi, A. Shafiee, V. Azizkhani, L. Dolatyari and S. W. Joo, Green Oxidation of Alcohols by Using Hydrogen Peroxide in Water in the Presence of Magnetic Fe3 O4 Nanoparticles as Recoverable Catalyst, *Green Chem. Lett. Rev.*, 2014, **7**(3), 257–264, DOI: **10.1080/17518253.2014.939721**.

21 G. Zhan, Y. Hong, F. Lu, A.-R. Ibrahim, M. Du, D. Sun, J. Huang, Q. Li and J. Li, Kinetics of Liquid Phase Oxidation of Benzyl Alcohol with Hydrogen Peroxide over Bio-Reduced Au/TS-1 Catalysts, *J. Mol. Catal. A: Chem.*, 2013, **366**, 215–221, DOI: **10.1016/j.molcata.2012.09.026**.

22 V. A. Matsura, V. V. Potekhin and V. B. Ukraintsev, Kinetics of Hydrogenation and Oxidation of Benzyl Alcohol in the Presence of Colloid Palladium *in situ*, *Russ. J. Gen. Chem.*, 2002, **72**(1), 105–109, DOI: **10.1023/A:1015309815764**.